Characterization of micro- to macroscopic deformation behavior of amorphous polymer with heterogeneous distribution of microstructures

Tomita, Yoshihiro

Uchida, Makoto

(Citation)
International Journal of Mechanical Sciences,45(10):1703-1716

(Issue Date)
2003-10

(Resource Type)
journal article

(Version)
Accepted Manuscript

(URL)
https://hdl.handle.net/20.500.14094/90000009

Characterization of Micro- to Macroscopic Deformation Behavior of Amorphous Polymer with Heterogeneous Distribution of Microstructures

Yoshihiro Tomita[1] and Makoto Uchida[2]

[1, 2] Graduate School of Science and Technology, Kobe University,

Nada Kobe, Japan 657-8501

Fax: +81-78-803-6155 tomita@mech.kobe-u.ac.jp

KEYWORDS: Amorphous Polymer, Distribution of Initial Shear Strength, Microscopic Shear Band, Macroscopic Shear Band, Molecular Chain Network Theory, Computational Simulation

ABSTRACT

In the present study, we clarify the micro- to macroscopic deformation behavior of an amorphous polymer with a slightly heterogeneous distribution of molecular chains, in other words, the distribution of the initial shear strength of the polymer. The micro- to macroscopic deformation behaviors of polymer under macroscopically uniform tension and shearing, uniaxial extension of a plane strain block and surface deformation of the plane strain block under compression were investigated by means of computational simulation with the nonaffine molecular chain network model. The results revealed the onset of microscopic shear bands emanating from slightly weak points and their evolution, and the interaction and percolation of new shear bands. The effects of distribution patterns and standard deviation of initial shear strength on the deformation, the interaction of weak points, the transition from microscopic shear band formation to macroscopic neck propagation and the evolution of surface undulation under compression have been demonstrated.

1. INTRODUCTION

The deformation behavior of polymeric materials under tension is very different from that of metallic materials. The plastic flow in an amorphous polymer that deforms due to the onset and growth of shear bands is initiated at a stress level lower than the macroscopic yielding point[1]. Such shear bands in an amorphous polymer are oriented along a direction very close to the direction of maximum shear stress. Subsequently, many shear bands form with the increase of deformation. Beyond the macroscopic yield point, shear bands are transformed into the macroscopically manifested neck and its propagation under the essentially steady state as often observed in experiments. These typical deformation behaviors are closely related to the heterogeneity of the microstructure of the amorphous polymer.

In order to reproduce the characteristic feature of the deformation behavior, a general three-dimensional constitutive model was established based on the three-chain model [2] using the generalized Argon's double-kink model [3] and the stress-strain relation for the perfect chain established by James and Guth [4]. Further generalizations of the model to the eight-chain model [5] and the full network model [6] have been performed. In those models, the polymeric material is approximated by a molecular chain network system defined by the cross-links, which are assumed to be physically entangled points of molecular chains, the number of which remains constant during the deformation. Therefore, these models are referred to as affine models. On the other hand, experimental investigations implicitly suggest the possibility of a change in the configuration of the entangled points due to deformation and a change in temperature [7,8], which causes a change in the rigidity of the polymeric materials. To accommodate this experimental evidence, a nonaffine model [9,10] based on the molecular chain network theory with the eight-chain model was established. Furthermore, the microstructure of amorphous polymer is expected to be highly heterogeneous, nevertheless, the discussions associated with this evidence are few [11], but in them, the distribution of strength with double peaks in low and high strength regions is introduced and the nonlinear deformation behavior before macroscopic yielding, the reverse loading processes and other mechanical characteristics are clarified.

In this paper, the characteristic deformation behavior of amorphous polymer is numerically specified by employing a nonaffine molecular chain network model and finite element simulation of

the amorphous polymer with a slightly heterogeneous chain distribution which was replaced by the heterogeneous initial shear strength. So far, information associated with the concrete distributions of chain density or the initial shear strength is not available, therefore, the distribution of shear strength is specified such that, depending on the total number of finite elements, a specific value of shear strength is allocated to an element and the number of elements with specific values of shear strength exhibits a normal distribution. The micro- to macroscopic deformation behavior of a unit cell under uniform tension and shearing, the effect of distribution patterns and standard deviation of initial shear strength on the deformation, and uniaxial tension of a plane strain block, including macroscopic neck propagation and the evolution of undulation of stress free surface of blocks under plane strain compression, will be discussed.

2. CONSTITUTIVE EQUATION

The complete constitutive equation for a polymer employed in this investigation is given in references [9,10]. Here, we provide a brief explanation of the constitutive equation. The total strain rate is assumed to be decomposed into the elastic strain rate and the plastic strain rate. The elastic strain rate is expressed by Hooke's law and the plastic strain rate is modeled using a nonaffine eight-chain model[9]. The final constitutive equation that relates the rate of Kirchhoff stress $\dot{S}_{ij}$ to strain rate $\dot{\varepsilon}_{kl}$ becomes

$$\dot{S}_{ij} = L_{ijkl}\dot{\varepsilon}_{kl} - P'_{ij}, \quad L_{ijkl} = D^{e}_{ijkl} - F_{ijkl}, \quad F_{ijkl} = \frac{1}{2}\left(\sigma_{ik}\delta_{jl} + \sigma_{il}\delta_{jk} + \sigma_{jl}\delta_{ik} + \sigma_{jk}\delta_{il}\right)$$

$$P'_{ij} = D^{e}_{ijkl}\frac{\dot{\gamma}^{p}}{\sqrt{2}\tilde{\tau}}\hat{\sigma}'_{kl}, \quad \tilde{\tau} = \left(\hat{\sigma}'_{ij}\hat{\sigma}'_{ij}/2\right)^{1/2}, \quad \hat{\sigma}_{ij} = \sigma_{ij} - B_{ij} \quad , \tag{1}$$

where D^{e}_{ijkl} is the elastic stiffness tensor and σ_{ij} is the Cauchy stress. The shear strain rate $\dot{\gamma}^{p}$ in Eq. (1) is given as [3]

$$\dot{\gamma}^{p} = \dot{\gamma}_{0}\exp\left[\left(-\frac{A\tilde{s}}{T}\right)\left\{1-\left(\frac{\tilde{\tau}}{\tilde{s}}\right)^{5/6}\right\}\right], \tag{2}$$

where $\dot{\gamma}_{0}$ and A are constants, T is the absolute temperature, $\tilde{\tau}$ is the applied shear stress, $\tilde{s} = s + ap$ indicates shear strength [2], s is the shear strength which changes, with plastic strain,

from the athermal shear strength $s_0 = 0.077\mu/(1-\nu)$ to a stable value s_{ss}, p is the pressure, a is a pressure-dependent coefficient, μ is the elastic shear modulus and ν is Poisson's ratio. Since s depends on the temperature and strain rate, the evolution equation of s can be expressed as $\dot{s} = h\{1-(s/s_{ss})\}\dot{\gamma}^p$, where h is the rate of resistance with respect to plastic strain. Furthermore, B_{ij} in Eq. (1) is the back-stress tensor and the principal components are expressed by employing the eight-chain model [5,6], as

$$B_i = \frac{1}{3}C^R\sqrt{N}\,\frac{V_i^2-\lambda^2}{\lambda}\,L^{-1}\left(\frac{\lambda}{\sqrt{N}}\right),$$

$$L(x) = \coth x - \frac{1}{x},\quad \lambda^2 = \frac{1}{3}(V_1^2+V_2^2+V_3^2), \tag{3}$$

where V_i is the principal plastic stretch, N is the average number of segments in a single chain, $C^R = nkT$ is a constant, n is the number of chains per unit volume, k is Boltzmann's constant, and L is the Langevin function. In the nonaffine eight-chain model [9,10], the change in the number of entangled points, in other words, the average number of segments N, may change depending on the temperature change and distortion ξ which represents the local deformation of a polymeric material. The variable ξ that reflects the change in the relative angle of the coordinate axes with unit base vectors $\boldsymbol{g}_i$ which are embedded parallel to the directions of principal plastic stretch in the initial stage of plastic deformation and deform into $\boldsymbol{G}_i$ by the subsequent deformation. For volume-constant deformation, $\xi = 1/(|\boldsymbol{G}_1||\boldsymbol{G}_2||\boldsymbol{G}_3|)$. The simplest version of the expression of the number of entangle points is $m = m_r \exp\{-c(1-\xi)\}$ with $\xi = 1$ in the reference state and m_r is the number of entangled points at reference state and c is a material constant[9,10].

3. COMPUTATIONAL MODEL

Here, we evaluate the detailed characteristics of micro- to macroscopic deformation of an amorphous polymer with heterogeneously distributed molecular chains. The distribution of molecular chains on a macroscopic scale is expected to be uniform, which is experimentally verified by measuring the tension of strips that were prepared from the polymer plate with different

directions. However, very localized deformation, in the form of microscopic shear bands, is observed in the initial stage of deformation, and subsequently, these bands develop and unify into macroscopic shear bands. The detailed characteristic feature of these deformation behaviors is clarified by careful observation [12,13] using an Atomic Force Microscope (AFM) under macroscopically uniform tension and shearing. Furthermore, large scale Molecular Dynamic (MD) simulation [14] suggested a heterogeneous distribution of the molecular chains. Nevertheless, the information associated with the concrete distributions of chain density or initial strength is not available, therefore, we restrict our investigations to the effect of the distribution of initial shear strength on the micro- to macroscopic deformation behavior of amorphous polymer, and will employ the normal distribution of the initial shear strength of the polymer.

The discussions in this paper will clarify the characteristic features of the deformation behavior of an amorphous polymer under macroscopically uniform/nonuniform deformation. The three models shown in Figs.1 (a), (b) and (c) are prepared for the investigation of the plane strain micro- to macroscopic deformation behavior, respectively. Uniform quadrilateral finite element discretization has been employed for (a) and (b), in which each quadrilateral consists of four crossed-triangular elements. To capture the localized surface deformation, the size of the elements increases exponentially from the top surface to the bottom for (c). The total number of quadrilaterals for (a), (b) and (c) are 80X80, 80X320 and 80X200, respectively. Figure 1 (a) illustrates the plane strain computational unit cell model for macroscopically uniform tension and shearing in which heterogeneous distribution of the initial shear strength of polymer s_0 is assumed. The distribution of s_0 is assumed instead of the chain density distribution. Figure 1(d) indicates the normal distribution of s_0 with mean value s_{0m}. The distribution of s_0 is specified such that, depending on the total number of finite elements in a unit cell, a specific value of s_0 is allocated to a square element and the number of elements with specific values of s_0 exhibits a normal distribution, as indicated in Fig.1 (d). Figure 1 (b) indicates the computational model for investigating the macroscopically nonuniform plane strain deformation including neck propagation. Figure.1 (c) indicates the computational model used to investigate the surface morphology of the block under plane strain uniform compression. The uniform end displacements shown in Fig. 1 (a), the uniform tension in (b) and uniform horizontal compression in (c) are applied. In all cases,

except for simple shear deformation, shear free conditions are applied to the surface of the boundary.

Here, we discuss the effects of the distribution of s_0 on macroscopic deformation behavior such as the average stress-strain relationship and neck propagation, and microscopic deformation behavior such as onset and propagation of the microscopic shear bands, and their unifications. Moreover, we define the average strain rates $\dot{E}_1, \dot{E}_2$ or stress rates $\dot{\Sigma}_1, \dot{\Sigma}_2$ with respect to the coordinate directions x_1, x_2, respectively, and macroscopic equivalent stress and strain are defined as $\Sigma_e = (3\Sigma_i^{'}\Sigma_i^{'}/2)^{1/2}$ and $E_e = (2E_i^{'}E_i^{'}/3)^{1/2}$ for the case of macroscopically uniform deformation. For the model in Fig.1(a), a macroscopically homogeneous strain rate $\dot{E}_e = \dot{\varepsilon}_0 = 10^{-5}/s$ is applied, whereas it is prescribed as $\dot{u}/L_0 = 10^{-5}/s$ and $\dot{u}/W_0 = 10^{-5}/s$ for the cases of Figs.1 (b) and (c), respectively. Since strain rate is sufficiently low, here we disregard the heat generation due to irreversible work. The material parameters for the polymer employed are $E_m/s_{0m} = 23.7$, $s_{ss}/s_{0m} = 0.79$, $h/s_{0m} = 5.15$, $As_{0m}/T_0 = 78.6$, $\alpha = 0.08$, $\dot{\gamma}_0 = 2.0\times10^{15}/s$, $s_{0m} = 97MPa$, $T_0 = 296K$, $m_0 = 7.83\times10^{26}$ and $c = 0.33$ [9,10], which are the modified versions of those for the affine eight-chain model [3,5]. Standard deviation (S.D.) for the normal distribution of initial shear strength is specified as $0.15s_{0m}$ for the cases unless noted otherwise.

4. RESULTS AND DISCUSSION

We first focus our attention on the investigation of the effect of the distribution of initial shear strength on the micro- to macroscopic deformation behavior of unit cells under uniform tension and shearing. The effect of the distribution pattern and S.D. on the deformation behavior, and the problems associated with the macroscopically nonuniform deformation due to microscopically heterogeneous plane strain deformation, including uniaxial tension with macroscopic neck propagation and surface undulation of blocks under compression, are further discussed.

4.1 Macroscopically Uniform Deformation

We will first discuss the micro- to macroscopic deformation behavior under uniform tension. Figures 2 (a), (b) and (c) respectively show the macroscopic stress to strain relations,

equivalent strain rate distribution on a unit cell and region A for tension. For comparison, the result for the homogeneous distribution of s_0 is also indicated in (a). The effects of microscopic distribution of s_0 is substantial in the early stage of deformation. The yield due to heterogeneous distribution of s_0 causes the nonlinear response prior to the macroscopic yield and suppresses 20% of the corresponding macroscopic yield stress in the homogeneous case. Furthermore, continuous yielding at different position of the polymer results the rather moderate increase of average stress with deformation as compared with the homogeneous case. However, the critical stretch is assumed to be identical in this investigation, therefore, the resistance of the deformation in the later stage asymptotically approaches that of the homogeneous case.

Figures 2 (b) and (c) indicate that the localized microscopic shear bands which connect the microscopically weak regions, appear at almost 45 degrees with respect to the tension direction. The macroscopic yield occurs at (3) where the microscopic shear bands cross the unit cell, which is responsible for lowering the yield stress as compared with the homogeneous case. Since the shear strength becomes s_{ss} in the region with a lower value of s_0, further softening may not occur. As a result, the strain rate in the initially formed shear bands possesses the maximum value at the macroscopic yielding point and it decreases with orientation hardening. The softening occurring in the subsequently generated microscopic shear band is compensated with hardening in the previously appearing shear band. Therefore, the stress vs strain relation for the unit cell in (a) exhibits no softening. With additional macroscopic deformation, the percolation, intensification and propagation of shear bands along the direction normal to the shear bands are observed, accompanied by the rotation of shear bands. Subsequently, the increase of the number of shear bands in which the maximum stretch attains the critical value, results in a significant increase of the resistance of deformation. The corresponding strain rate distribution is seen in (8) of Fig.2 (c) which indicates almost uniform deformation.

A similar behavior as observed in the case of tension can be seen in the case of shearing except for the direction of the shear band, which depends on the principal shear direction. Figures 3 (a) and (b) indicate the corresponding results for shearing of the unit cells. Since the maximum shear directions are horizontal and vertical for the case of shearing, the shear bands corresponding directions evolve and propagate. With regard to the effect of the heterogeneous distribution of the

shear strength on the energy consumption during deformation, higher energy is generally required for the heterogeneous case.

4.2 Effect of Distribution Pattern of Initial Shear Strength on Deformation Behavior

Due to the lack of suitable information on the concrete distribution of the initial shear strength, the discussion has been restricted to the normal distribution with a specific S.D. of the initial shear strength. However, the distribution pattern of the initial shear strength of the molecular chain may affect the deformation behavior. Therefore, we will focus our attention on the effect of the S.D. and the profile of the heterogeneous distribution pattern of initial shear strength on the deformation behavior.

Figure 4 indicates (a) macroscopic equivalent stress-strain relations and (b) equivalent strain rate distributions for the cases with S.D. of $0.00s_{0m} - 0.15s_{0m}$. With the increase of the S.D. of the initial shear strength, the number of areas possessing lower and higher initial shear strengths increases. The former causes the onset of shear bands in the early stage of deformation, which results in the nonlinear response and lowering of the macroscopic yield stress, as depicted in Fig. 4(a). Furthermore, the difference between the initial shear strength s_0 and its stable value s_{ss} decreases, which causes orientation hardening shortly after softening. This contributes to the increase of the resistance to deformation. On the other hand, the onset of shear band with softening in areas with a higher value of the initial shear strength is retarded. All these contribute to postponing the asymptotic approach to the homogeneous case. However, as can be seen in Fig. 4, the effect of the magnitude of S.D. of the initial shear strength on the microscopic as well as macroscopic deformation is rather small. The results suggest that the existence of heterogeneity is essential for the occurrence of local deformation.

Figure 5 indicates the effect of the distribution pattern of the initial shear strength on the micro- to macroscopic deformation behavior of amorphous polymer. The β distribution with the same average value of the initial shear strength, as indicated in Fig.5(a), was introduced. Figures 5(b) and (c) respectively indicate the macroscopic stress vs strain relations and corresponding equivalent strain rate distribution at the macroscopic equivalent strain indicated in Fig.5(b). The effect of the location of maximum initial shear strength on the micro- to macroscopic deformation behavior is not substantial.

According to the results obtained, the investigation based on the normal distribution with a specific S.D. of the initial shear strength may provide a general perspective of the deformation behavior of amorphous polymer with a heterogeneous distribution of the initial shear strength.

4.3 Uniaxial Tension of Plane Strain Block

Figure 6 indicates the deformation behavior of block subjected to plane strain tension. Here, we will discuss the effect of the magnitude of the standard deviation (S.D.) of the initial shear strength on the micro to macroscopic deformation behavior. Figure (a) shows the nominal stress vs nominal strain relation for three different S.D. values of the initial shear strength. Figure 6 (b) shows the corresponding strain rate distributions at the points indicated in (a). Typical macroscopic deformation behaviors are reproduced for the case of small S.D. As can be seen in the figure, before the onset of macroscopic yield, the microscopic concentration of deformation began as in the case of macroscopically homogeneous deformation. Furthermore, the effect of heterogeneity on the macroscopic yield is rather small for the case of a small S.D. of the initial shear strength, whereas its effect in the later stage of deformation is very prevalent and the energy consumption during deformation is increased, as in the case of macroscopically uniform deformation.

Figure 6 (b) indicates the plastic strain rate distribution for the case of different S.D. values of the initial shear strength. In the figure, (1)-(8) and (i)-(viii) indicate the location depicted in the macroscopic nominal stress vs strain relation. Macroscopic yielding occurs immediately after the microscopic shear band intersects the cross section of the specimen. Subsequently, the macroscopic force dropped markedly when softening occurred in the specific shear band in the case of a low S.D. of the initial shear strength. With the increase of the S.D. of the initial shear strength, due to the continuous yield caused by the heterogeneous distribution of shear strength, the nonlinear behavior observed before macroscopic yielding is promoted and a subsequent drop of the resistance is suppressed. With further deformation, orientation hardening occurs in the shear bands, which causes the propagation of shear bands in the direction normal to the shear bands and the percolation of new shear bands accompanied by the propagation of macroscopic neck along the tension direction. Due to the computational condition, macroscopic necks developed initially at the both ends, therefore, a rather special deformation processes are observed. Nevertheless, the deformation

behavior of the half specimen represents the experimentally observed evidence. The size of macroscopic neck depends substantially on the magnitude of the S.D. of the initial shear strength. It increases with decreasing of S.D. of the initial shear strength, which results in the marked drop of the resistance of deformation. It should be noted that very clear shear bands develop in the unnecked parts. The shear bands in the necking area exhibit curvature due to the macroscopically nonuniform deformation caused by necking and the average stress changes along the curved shear bands as can be seen in slip-line fields of rigid-plastic materials. In macroscopically uniform deformation cases, the microscopic shear bands are essentially straight and the average stress remains almost unchanged throughout the shear band.

4.4 Compression of Plane Strain Blocks

Figures 7 (a) and (b) respectively indicate the macroscopic nominal stress vs. nominal strain relation and the strain rate distribution and (c) depicts the evolution of surface undulation for the plane strain blocks due to inhomogeneous deformation caused by the distribution of s_0 under macroscopically uniform compression. A significant increase in the undulation starts where micro shear bands connecting weak points develop, and subsequently, the rate of increase of undulation decreases, different from the case of metallic materials[15]. This is due to the characteristic feature of the polymeric materials, which is caused by orientation hardening. More precise observation clarified that in the initial stage of deformation, the onset of long wavelength undulation is predominant and is sharpened with further deformation. Subsequently, due to the orientation hardening the evolution of long wave length undulation is suppressed. With further deformation, onset, propagation and percolation of microscopic shear bands cause the additional short wavelength surface undulation which can be clearly seen in the magnified image of the surface of the block in Fig.7(c). That is to say, the wavelength of undulation changes with the straining. Undulation with a long wavelength initially appears, and subsequently, short wavelength undulations are manifested. The surface undulations are governed by the intersection of shear bands on the surface of the block where deformation is restrained due to orientation hardening. Therefore, these intersection points of shear bands act as nodes of undulation. This is clearly shown by the Fourier transformation of the surface profile. Figures 8(a) and (b) respectively correspond to the amplitude of surface undulation of the initial and a later stage of deformation. The numbers in the

figure correspond to deformation stages in Fig.8(a). In the initial stage of deformation, the onset of the long wavelength undulation is predominant and is sharpened with further deformation. In the later stage of deformation, on the other hand, due to orientation hardening, the growth of long wavelength undulation is suppressed. Further onset and propagation, and percolation of micro shear bands causes the additional short wavelength undulation. These characteristic deformation behaviors qualitatively reproduce the main feature captured in AFM observation of the surface of PC under deformation [12,13].

5. CONCLUSION

A series of computational simulations of the deformation behavior of an amorphous polymer with heterogeneous distribution of the initial shear strength clarified the characteristic features of the micro- to macroscopic deformation behavior. The results are summarized as follows.

(1) The distribution of the initial shear strength causes the onset of micro shear bands that connect the weak points, which causes the softening of the macroscopic stress and strain relations and nonlinear response before the start of macroscopic yielding.

(2) A nearly steady-state deformation, in which the resistance to deformation is almost constant, is attained during the propagation of microscopic shear bands in the direction normal to the micro shear bands, and the percolation of new shear bands. Termination of the propagation results in a significant upward trend in stress and strain relations.

(3) The effect of the magnitude of the standard deviation and the profile of the distribution of the initial shear strength on the microscopic as well as macroscopic deformation is rather small. Therefore, the investigation based on the normal distribution with a specific standard deviation of heterogeneity of the initial shear strength may provide a general overview of the deformation behavior of amorphous polymer.

(4) In tension of the plane strain block, macroscopic yielding occurs immediately after microscopic shear bands intersect the specimen, where a considerable drop of the macroscopic force occurs due to softening in the localization zone. With orientation hardening in the localization zone, locally similar behaviors as described in (1) and (2) are observed, which leads to macroscopic

neck propagation in the tension direction. It should be noted that very clear localized deformation zones are developed in the unnecked parts.

(5) The undulation caused by the nonuniform deformation due to the distribution of the initial shear strength manifests different features depending on the stage of deformation. The wavelength of the undulation decreases as the deformation proceeds, which is caused by the onset, and propagation and the percolation of shear bands.

(6) In macroscopically homogeneous deformation as well as heterogeneous deformation, the deformation resistance increases with the existence of heterogeneity of the initial shear strength and therefore, energy consumption during the deformation increases as well.

ACKNOWLEDGMENT

Financial support from the Ministry of Education, Culture, Sports, Science and Technology of Japan is gratefully acknowledged.

REFERENCES

[1] Courtney, T. H.: *Mechanical Behavior of Materials* (1990) McGraw-Hill.

[2] Boyce, M. C., Parks, D. M. and Argon, A. S.: *Large inelastic deformation of glassy polymers, Part I: rate dependent constitutive model.* Mech. Mater., 1988. **7,**15-33.

[3] Argon, A. S.: *A theory for the low-temperature plastic deformation of glassy polymers.* Phil. Mag. 1973, **28**,839-865.

[4] James, H. M., Guth, E. J.: *Theory of the Elastic Properties of Rubber*. Chem. Phys., **11**, 455(1943)

[5] Arruda, E. M. and Boyce, M. C.: *A three-dimensional constitutive model for large stretch behavior of rubber materials.* J. Mech. Phys. Solids, 1993, **41**,389-412.

[6] Wu, P. D. and Van der Giessen, E.: *On improved network models for rubber elasticity and their applications to orientation hardening in glassy polymers.* J. Mech. Phys. Solids, 1993, **41**,427-456.

[7] Raha, S. and Bowden, P. B.: *Birefringence of plastically deformed poly (methyl methacrylate).*

Polymer, 1972, **13**,174-183.

[8] Botto, P. A., Duckett, R. A. and Ward, I. M.: *The yield and thermoelastic properties of oriented poly (methyl methacrylate).* Polymer , 1987, **28**, 257-262.

[9] Tomita, Y., Adachi, T., and Tanaka, S.: *Modelling and Application of Constitutive Equation for Glassy Polymer Based on Nonaffine Network Theory.* Eur. J. Mech. A/Solids, ,1997, **16**, 745-755.

[10] Tomita, Y. and Adachi, T.: *Nonaffine network model for glassy polymer and prediction of instability propagation,* T., De Borst, R and Van der Giessen, E., eds. Proc. IUTAM Symposium on Materials Instabilities, 1998, Wiley & Sons Ltd., 303-321.

[11] Boyce, M. C., and Chui, C.,:*Effect of heterogeneities and localization of polymer deformation and recovery,* T., De Borst, R and Van der Giessen, E., eds. Proc. IUTAM Symposium on Materials Instabilities, 1998, Wiley & Sons Ltd.,269-285.

[12] Kashu,Y., Adachi, T. and Tomita, Y.: *AFM observation of microscopic behavior of glassy polymer with application to understanding of macroscopic behavior.* Eds. Abe, T and Tsuta, T, Proc. AEPA'96 Pergamon, 1996, 501-505.

[13] Adachi, T., Tomita, Y., and Kashu, Y.: *AFM observation of microscopic behavior of glassy polymer under macroscopic tension,* Trans. JSME, 1998, **64A** ,758-764.(in Japanese)

[14] Itoh, T., Yashiro, K., and Tomita, Y., *Molecular dynamic study on deformation of molecular chains in amorphous polymer,* JSMS 7 th Symposium on Molecular Dynamics,(2002) 50-55.

[15] Tvergaard, V., *Influence of void nucleation on ductile shear fracture at a stress free surface*, J. Mech. Phys. Solids, 1982, **30**, 399-425.

Figure Captions

Figure 1 Computational Models

(a) Plane strain macroscopically uniform tension and shearing model with uniform 80X80 quadrilateral elements discretization.

(b) Plane strain tension block model with uniform 80X320 quadrilateral elements discretization.

(c) Plane strain compression block model with nonuniform 80X200 quadrilateral elements discretization. The size of elements increase exponentially from the surface of the block to the bottom.

(d) Normal distribution of initial shear strength

Figure 2 Macroscopically Uniform Tension

(a) Macroscopic equivalent stress vs strain

(b) Equivalent strain rate distribution

(c) Equivalent strain rate distribution on region A in (a)

Figure 3 Macroscopically Uniform Shearing

(a) Macroscopic equivalent stress vs strain

(b) Equivalent strain rate distribution

Figure 4 Effect of Standard Deviation of Initial Shear Strength on Deformation Behavior

(a) Macroscopic equivalent stress vs strain

(b) Equivalent strain rate distribution

Figure 5 Effect of Distribution Pattern of Initial Shear Strength on Deformation Behavior

(a) Distribution pattern of initial shear strength

(b) Macroscopic equivalent stress vs strain

(c) Equivalent strain rate distribution

Figure 6 Plane Strain Tension of Blocks with Different Standard Deviation of Initial Shear Strength.

(a) Nominal stress vs strain

(b) Equivalent strain rate distribution

Figure 7 Blocks with Free Surface under Plane Strain Compression

(a) Macroscopic nominal stress vs strain

(b) Equivalent strain rate distribution

(d) Evolution of surface undulation

Figure 8 Fourier Transformation of Surface Undulation

(a) Initial stage of deformation

(b) Later stage of deformation

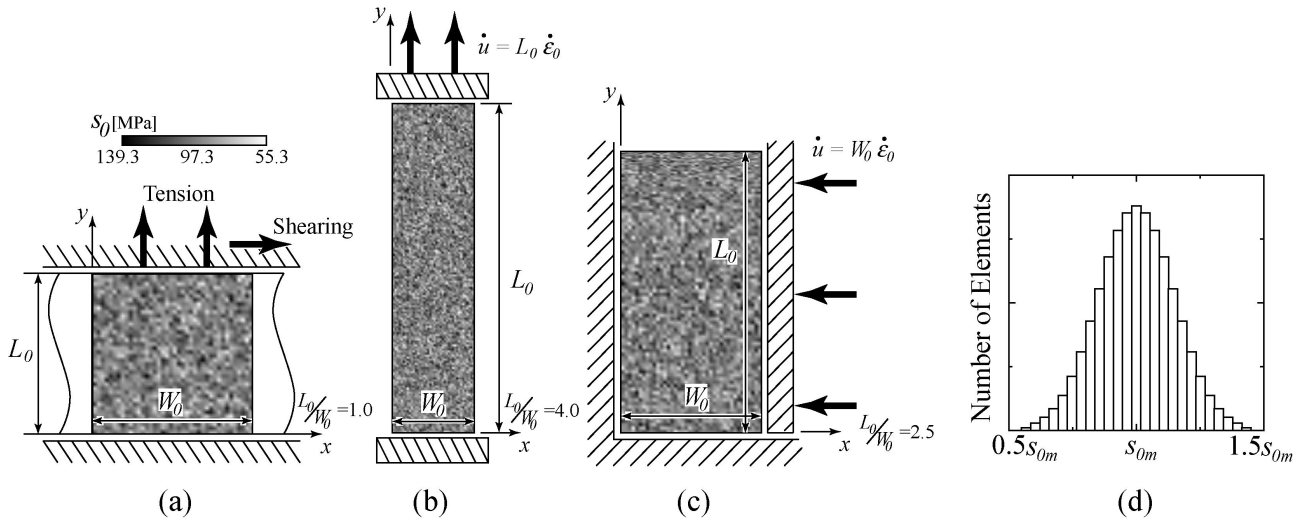
S_0[MPa]
139.3
97.3
55.3
Tension
Shearing
L_0
W_0
L_0/W_0 =1.0
$\dot{u} = L_0 \dot{\varepsilon}_0$
L_0/W_0 =4.0
$\dot{u} = W_0 \dot{\varepsilon}_0$
L_0/W_0 =2.5
Number of Elements
$0.5s_{0m}$
s_{0m}
$1.5s_{0m}$
(a)
(b)
(c)
(d)

Figure 1

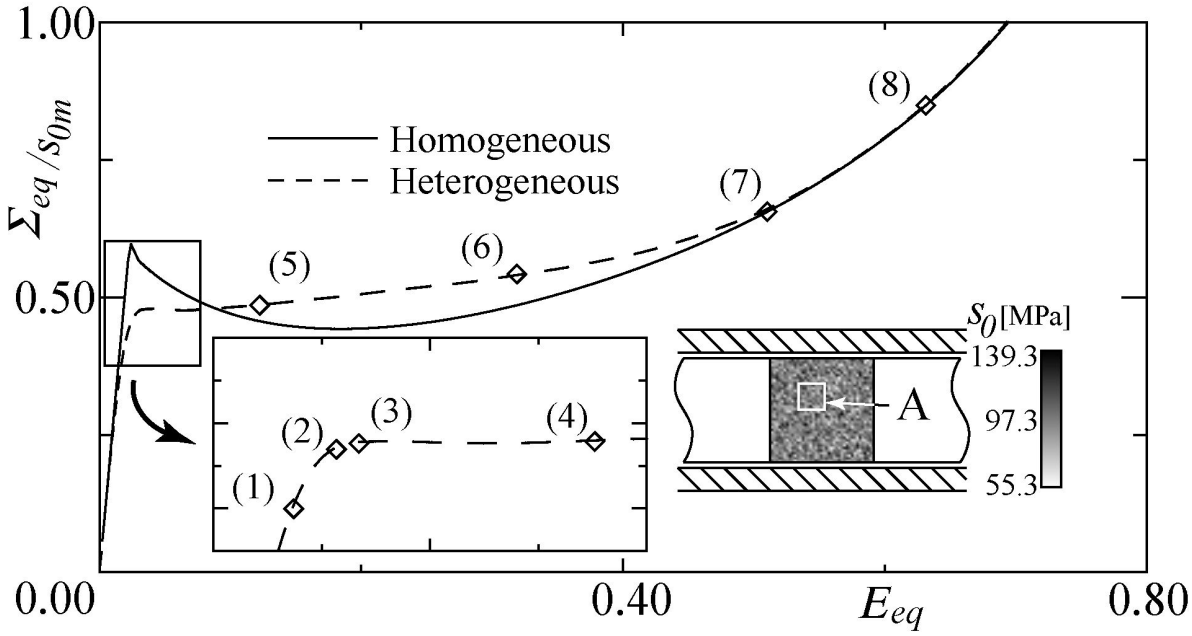
1.00
0.50
0.00
0.40
0.80
E_{eq}
Σ_{eq}/s_{0m}
Homogeneous
Heterogeneous
(1)
(2)
(3)
(4)
(5)
(6)
(7)
(8)
s_0[MPa]
139.3
97.3
55.3
A

(a)

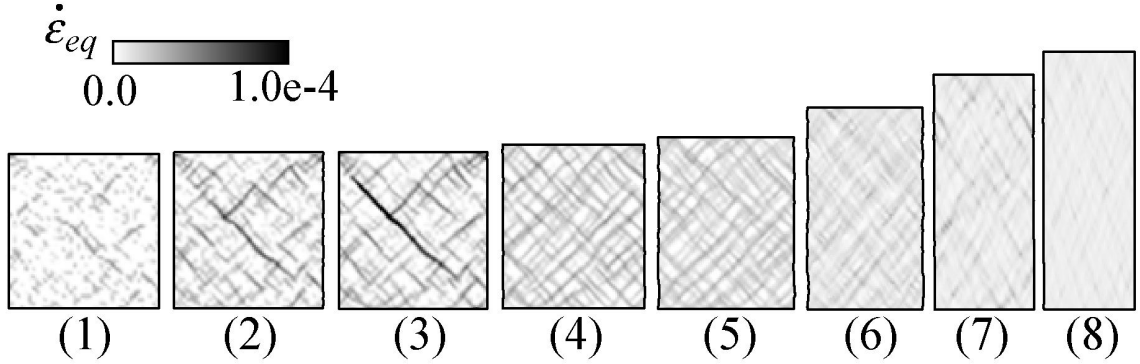
$\dot{\varepsilon}_{eq}$
0.0
1.0e-4
(1)
(2)
(3)
(4)
(5)
(6)
(7)
(8)

(b)

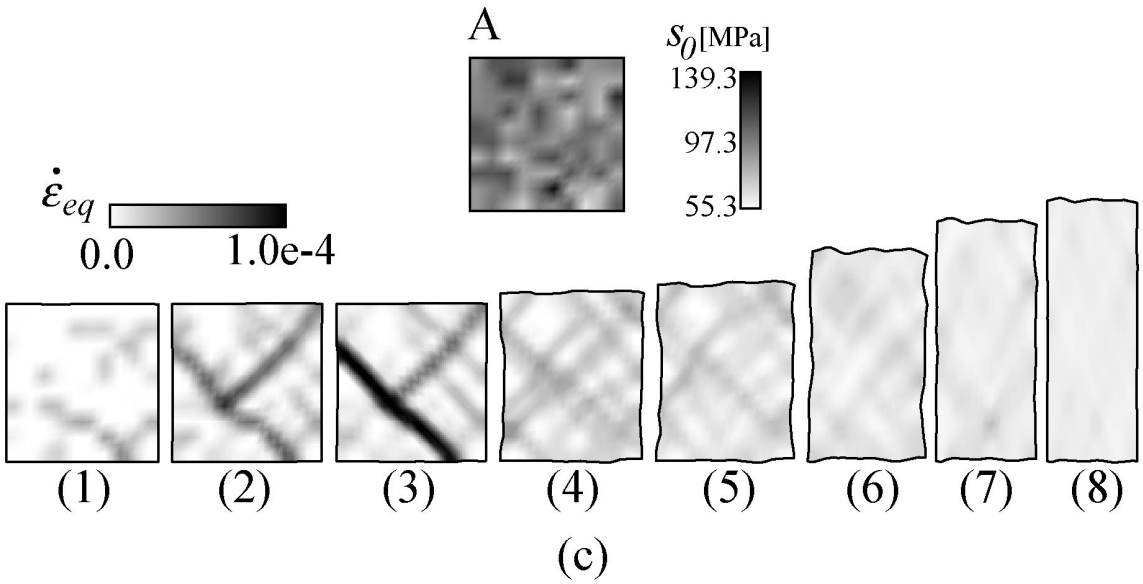
A
s_0[MPa]
139.3
97.3
55.3
$\dot{\varepsilon}_{eq}$
0.0
1.0e-4
(1)
(2)
(3)
(4)
(5)
(6)
(7)
(8)

(c)

Figure 2

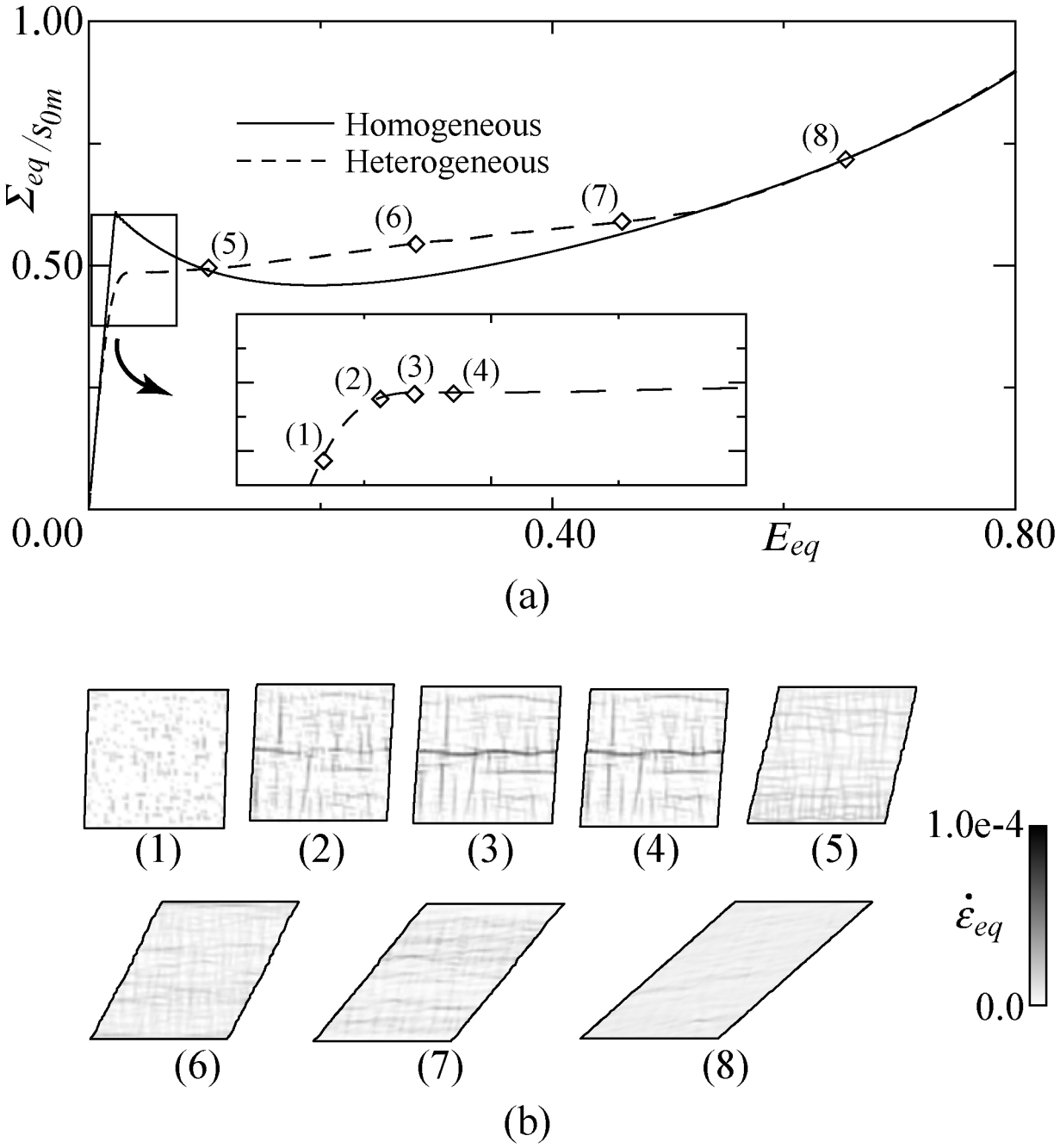
1.00
0.50
0.00
0.40
0.80
Σ_{eq}/s_{0m}
E_{eq}
Homogeneous
Heterogeneous
(1)
(2)
(3)
(4)
(5)
(6)
(7)
(8)
(a)
1.0e-4
$\dot{\varepsilon}_{eq}$
0.0
(b)

Figure 3

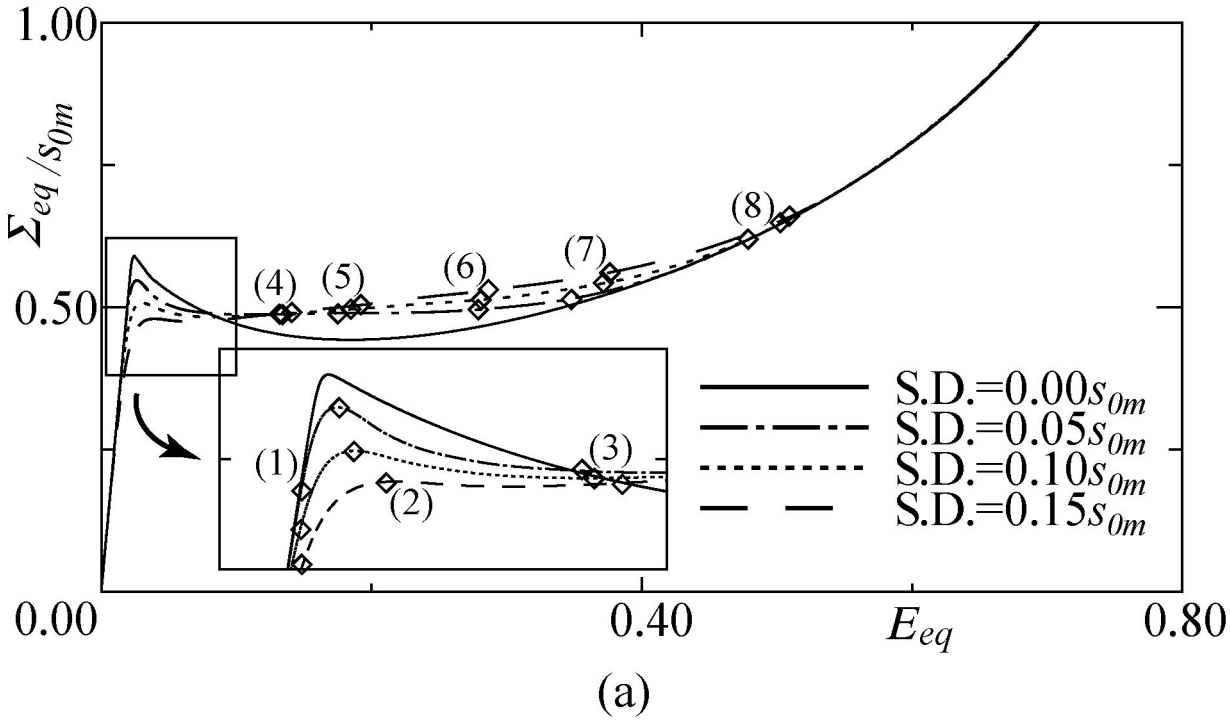
1.00
0.50
0.00
0.40
0.80
Σ_{eq}/s_{0m}
E_{eq}
(1)
(2)
(3)
(4)
(5)
(6)
(7)
(8)
S.D.=0.00s_{0m}
S.D.=0.05s_{0m}
S.D.=0.10s_{0m}
S.D.=0.15s_{0m}

(a)

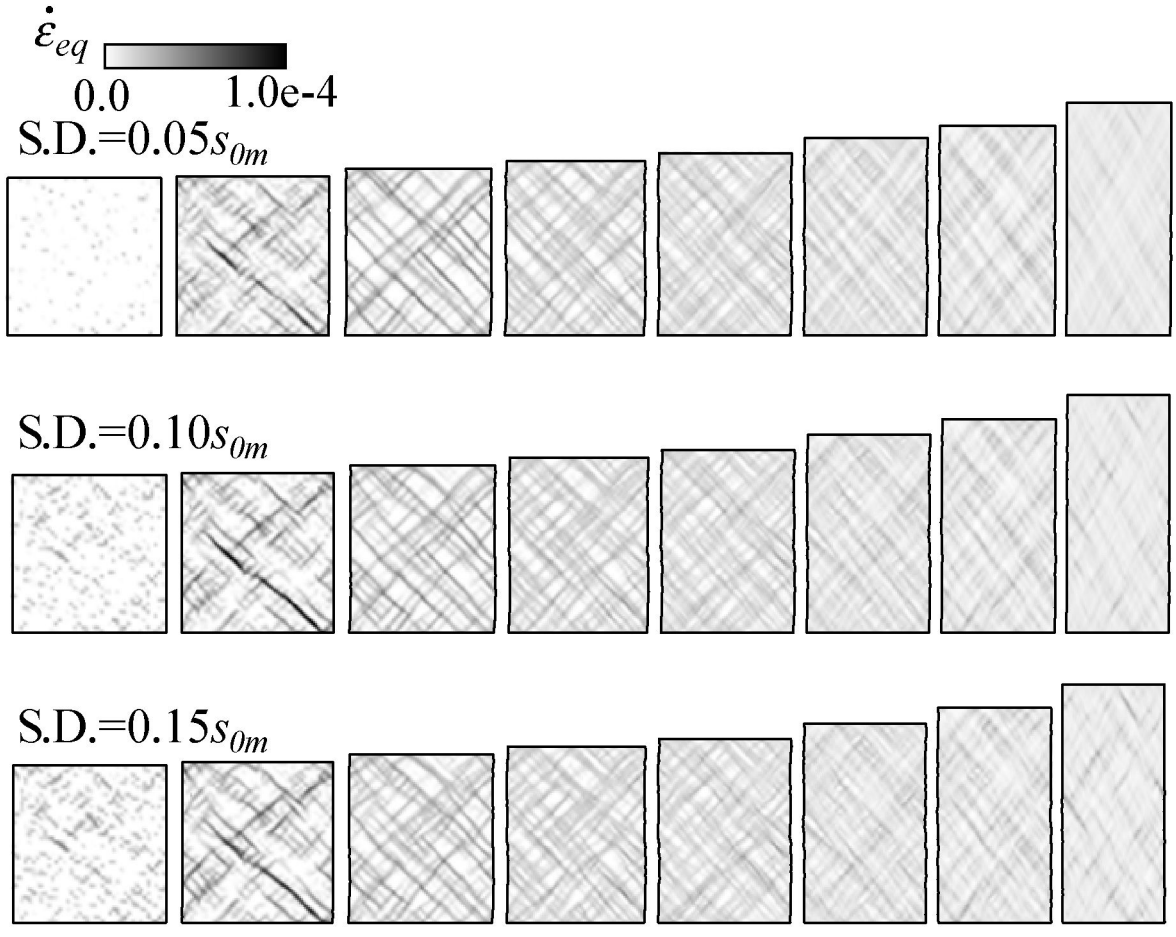
$\dot{\varepsilon}_{eq}$
0.0
1.0e-4
S.D.=0.05s_{0m}
S.D.=0.10s_{0m}
S.D.=0.15s_{0m}
(1)
(2)
(3)
(4)
(5)
(6)
(7)
(8)

(b)

Figure 4

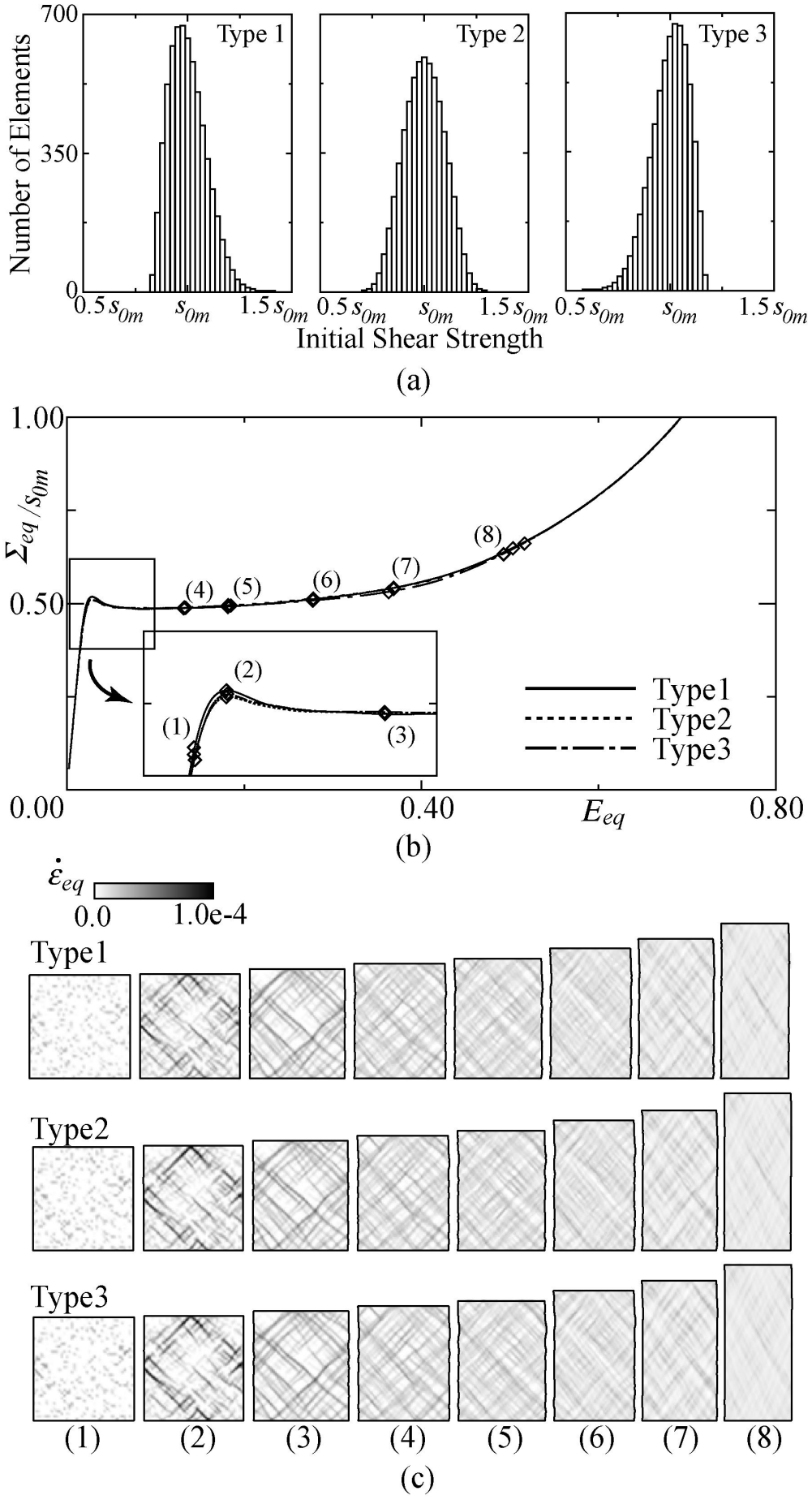
700
350
0
Number of Elements
Type 1
Type 2
Type 3
0.5 s_{0m}
s_{0m}
1.5 s_{0m}
Initial Shear Strength
(a)
1.00
0.50
0.00
Σ_{eq}/s_{0m}
(1)
(2)
(3)
(4)
(5)
(6)
(7)
(8)
Type1
Type2
Type3
0.40
E_{eq}
0.80
(b)
$\dot{\varepsilon}_{eq}$
0.0
1.0e-4
Type1
Type2
Type3
(1)
(2)
(3)
(4)
(5)
(6)
(7)
(8)
(c)

Figure 5

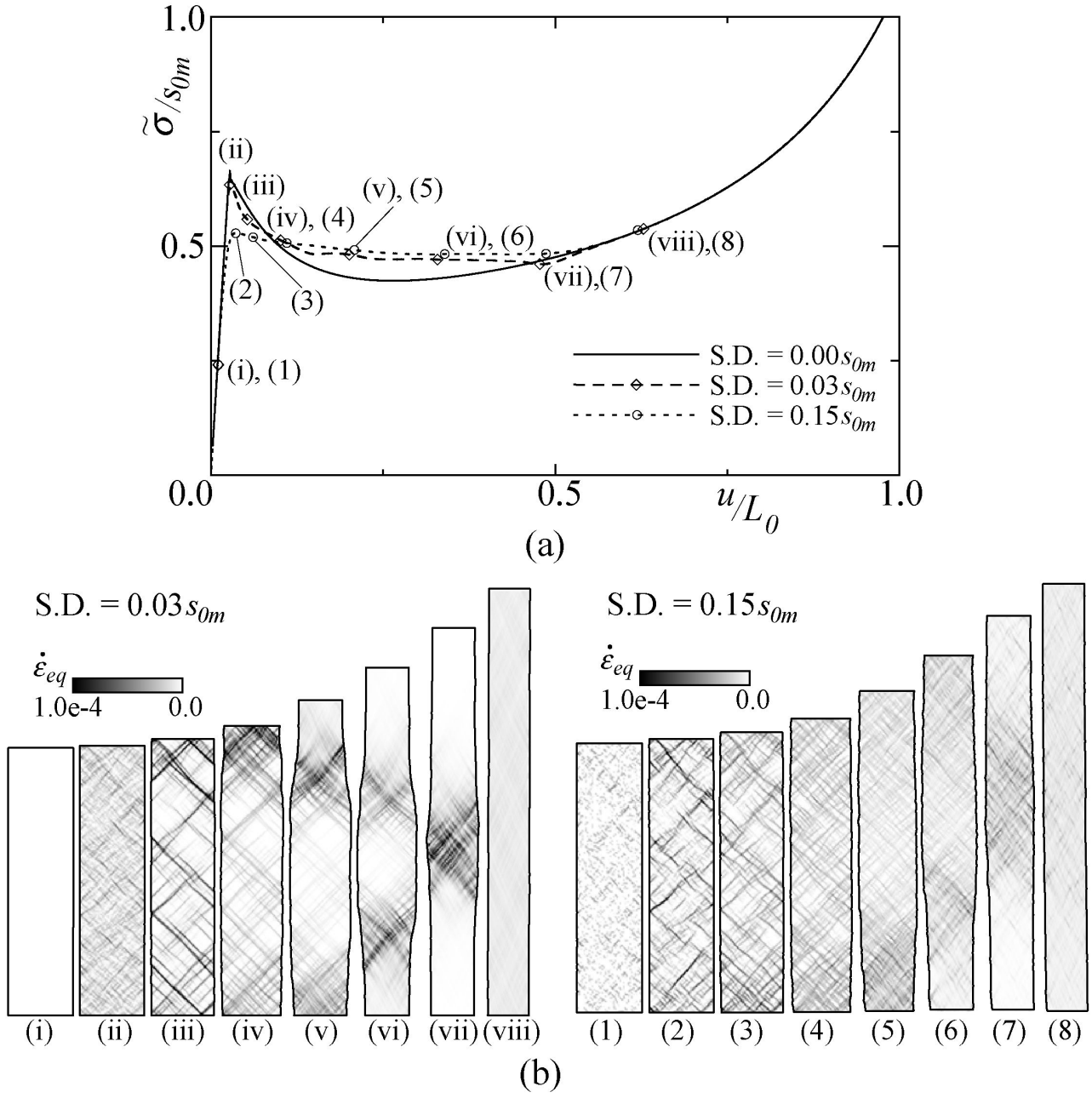
1.0
0.5
0.0
0.5
1.0
$\tilde{\sigma}/s_{0m}$
u/L_0
(i), (1)
(ii)
(iii)
(iv), (4)
(v), (5)
(vi), (6)
(vii),(7)
(viii),(8)
(2)
(3)
S.D. = $0.00s_{0m}$
S.D. = $0.03s_{0m}$
S.D. = $0.15s_{0m}$
(a)
S.D. = $0.03s_{0m}$
$\dot{\varepsilon}_{eq}$
1.0e-4
0.0
S.D. = $0.15s_{0m}$
$\dot{\varepsilon}_{eq}$
1.0e-4
0.0
(i)
(ii)
(iii)
(iv)
(v)
(vi)
(vii)
(viii)
(1)
(2)
(3)
(4)
(5)
(6)
(7)
(8)
(b)

Figure 6

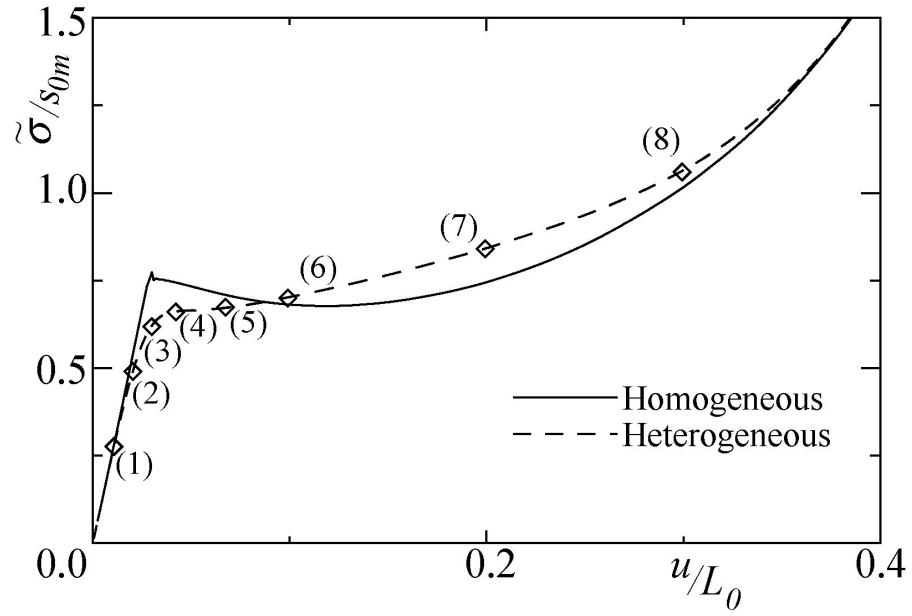
1.5
1.0
0.5
0.0
0.2
0.4
$\tilde{\sigma}/s_{0m}$
u/L_0
(1)
(2)
(3)
(4)
(5)
(6)
(7)
(8)
Homogeneous
Heterogeneous

(a)

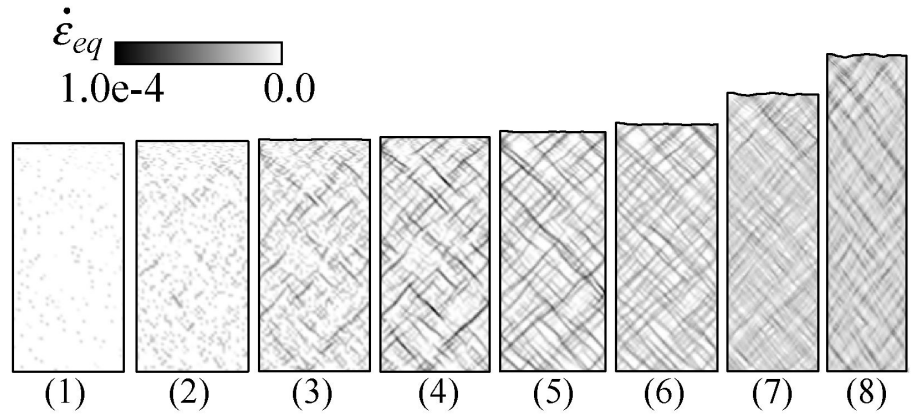
$\dot{\varepsilon}_{eq}$
1.0e-4
0.0
(1)
(2)
(3)
(4)
(5)
(6)
(7)
(8)

(b)

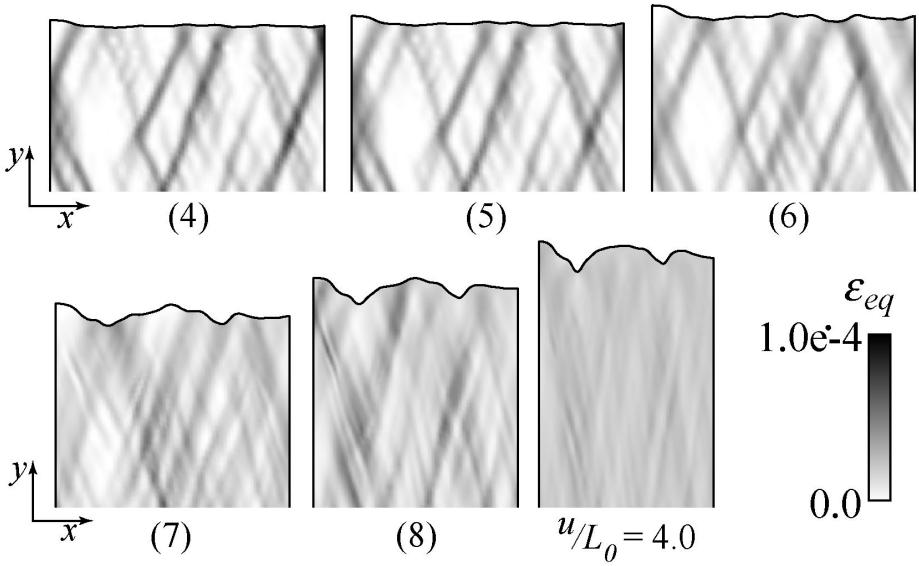
y
x
(4)
(5)
(6)
(7)
(8)
$u/L_0 = 4.0$
ε_{eq}
1.0e-4
0.0

(c)

Figure 7

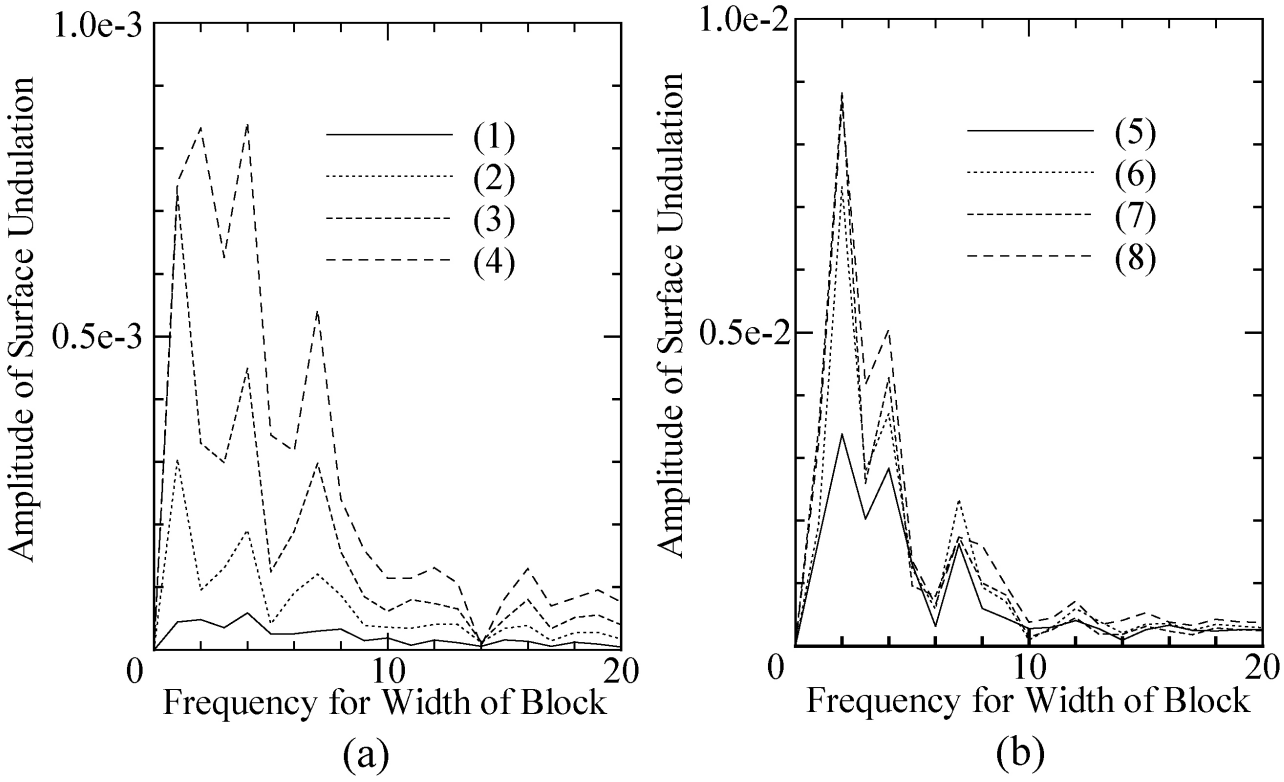
1.0e-3
0.5e-3
0
10
20
Amplitude of Surface Undulation
Frequency for Width of Block
(1)
(2)
(3)
(4)
(a)
1.0e-2
0.5e-2
0
10
20
Amplitude of Surface Undulation
Frequency for Width of Block
(5)
(6)
(7)
(8)
(b)

Figure 8